catalysts

MDPI

Article

Photocatalytic Performance of Functionalized Biopolymer for Neodymium (III) Sorption and the Recovery from Leachate Solution

Mohammed F. Hamza,[1,2,*] Hamed Mira[2], Mahmoud S. Khalafalla,[2] Ji Wang,[1*] Yuezhou Wei,[1,3], Xiangbiao Yin[1], Shunyan Ning [1], Khalid Althumayri[4], Amr Fouda[5]

[1]School of Nuclear Science and Technology, University of South China, Hengyang 421001, China; m_fouda21@usc.edu.cn (M.F.H.), yzwei@usc.edu.cn (Y.W.); ningshunyan@usc.edu.cn (S.N), yinxb@usc.edu.cn (XY), wangji@ usc.edu.cn (J.W)

[2]Nuclear Materials Authority, POB 530, El-Maadi, Cairo 11728, Egypt; m_fouda21@ usc.edu.cn (M.F.H.), hamedmira@yahoo.com (H.M), mahmoudsayed24@yahoo.com (M.S.K),

[3]School of Nuclear Science and Engineering, Shanghai Jiao Tong University, Shanghai 200240, China yzwei@usc.edu.cn (Y.W.)

[4]Department of chemistry, College of science, Taibah University, 30002 Al-Madinah Al-Munawarah, Saudi Arabia Kthumairi@taibahu.edu.sa (K.A)

Botany and Microbiology Department, Faculty of Science, Al-Azhar University, Nasr City, Cairo 11884, Egypt; amr_fh83@azhar.edu.eg (A.F.)

* Correspondence: m_fouda21@usc.edu.cn (M.F.H.); wangji@ usc.edu.cn (J.W); Tel.: +20-111-668-1228 (M.F.H.); +86-771-322-4990 (Y.W.)

Table S1. Assignment peaks of MCH, CH-POH, CH-POH+Nd and After 5 cycles of sorption desorption

Vibration	MCH	CH-POH	CH-POH+Nd	After 5 cycles	
O-H and N-H Str. (overlapped)	3412	3267	3274	3263	[7-1]
C-H aliph. (str.)	2928 ,2847	2917, 2848		2919, 2850	[12-8]
C=O (amide) and C=N- (overlapped) (str.)	1637	1691, 1621, 1552	1569	1698	[13,14]
1°/2° amines (bend)	1542			1575	[15,16]
C-H asym. (bend)	1380	1431	1396	1415	[17,18]
P=O (asym.)		1348		1370	[19,20]
O-H (in-plane) bend	1161	1261, 1236	1147	1311	[21,22]
P(O) (phosphate(str.))		1053	1126	1137	[19]
C-O, C-O-C and C-N (str.)	1019	1006	1024	1024	[23]
P-O-C (str.)		908	946, 890	892	[19]
-$(CH_2)n$- rocking	882	827	811	795	[24]
P-O-C (str.)		609	617	596	[19,20]
Fe-O	570	561		549	[25]

Table S2. Elemental analysis of MCH and CH-POH sorbents

	C	**N**	**H**	**O**	**Fe**	**P**
MCH [%]	27.35	4.12	5.06	30.22	33.25	0
MCH [m mol]	22.77	2.94	50.2	18.89	5.95	0
MCH-NPOH [%]	22.96	5.58	4.98	36.92	26.61	2.95
M MOL [m mol]	19.12	3.98	49.4	23.08	4.76	0.95

Table S3a. Reminder on equations used for modeling sorption isotherms [26-28].

Model	Equation	Parameters	Ref.
Langmuir	$q_{eq} = \frac{q_{m,L} C_{eq}}{1 + b_L C_{eq}}$	$q_{m,L}$ (mmol g^{-1}): Sorption capacity at saturation of monolayer b_L (L $mmol^{-1}$): Affinity coefficient	[26]
Freundlich	$q_{eq} = k_F C_{eq}^{1/n_F}$	k_F and n_F: empirical parameters of Freundlich equation	[26]
Sips	$q_{eq} = \frac{q_{m,S} b_S C_{eq}^{1/n_S}}{1 + b_S C_{eq}^{1/n_S}}$	$q_{m,L}$, b_S and n_S: empirical parameters of Sips equation (based on Langmuir and Freundlich equations)	[26]

Table S3b. Reminder on equations used for modeling uptake kinetics [26,29] [30].

Model	Equation	Parameters	Ref.
PFORE	$q(t) = q_{eq,1}(1 - e^{-k_1 t})$	$q_{eq,1}$ (mmol g^{-1}): sorption capacity at equilibrium k_1 (min^{-1}): apparent rate constant of PFORE	[30]
PSORE	$q(t) = \frac{q_{eq,2}^2 k_2 t}{1 + k_2 q_{eq,2} t}$	$q_{eq,2}$ (mmol g^{-1}): sorption capacity at equilibrium k_2 (g $mmol^{-1}$ min^{-1}): apparent rate constant of PSORE	[30]
RIDE	$\frac{q(t)}{q_{eq}} = 1 - \sum_{n=1}^{\infty} \frac{6\alpha(\alpha+1)\exp\left(\frac{-D_e q_n^2}{r^2} t\right)}{9 + 9\alpha + q_n^2 \alpha^2}$ With q_n being the non-zero roots of $\tan q_n = \frac{3\, q_n}{3 + \alpha q_n^2}$ and $\frac{m\, q}{V\, C_0} = \frac{1}{1+\alpha}$	D_e (m^2 min^{-1}) : Effective diffusivity coefficient	[29]

(m (g): mass of sorbent; V (L): volume of solution; C_0 (mmol L^{-1}): initial concentration of the solution).

Akaike Information Criterion, AIC:

$$AIC = N \ln\left(\frac{\sum_{i=0}^{N}\left(y_{i,exp.} - y_{i,model}\right)^2}{N}\right) + 2N_p + \frac{2N_p\left(N_p + 1\right)}{N - N_p - 1}$$

Where N is the number of experimental points, N_p the number of model parameters, $y_{i,exp.}$ and $y_{i,model}$ the experimental and calculated values of the tested variable.

Table S4. XRF analysis of the study ore materials.

Major oxides (%)	**Wt. (%)**	**Trace elements**	**ppm**
SiO_2	76.51	U	1117
Al_2O_3	8.56	REE	1296
TiO_2	0.95	Mn	35.4
$Fe_2O_3^{total}$	3.26	Zn	86.4
CaO	1.19		
MgO	0.45		
Na_2O	0.43		
K_2O	1.18		
P_2O_5	0.49		
L.O.I	5.68		
Total	98.7		

Table S5. Chemical composition of the prepared carbonate leach liquor at (pH=0.3)

Constituent	Conc. (mg/L)	Constituent	Conc. (mg/L)
Fe	2690	Ca	448
Al_2O_3	2538	U	388
Mg	350	REE	451

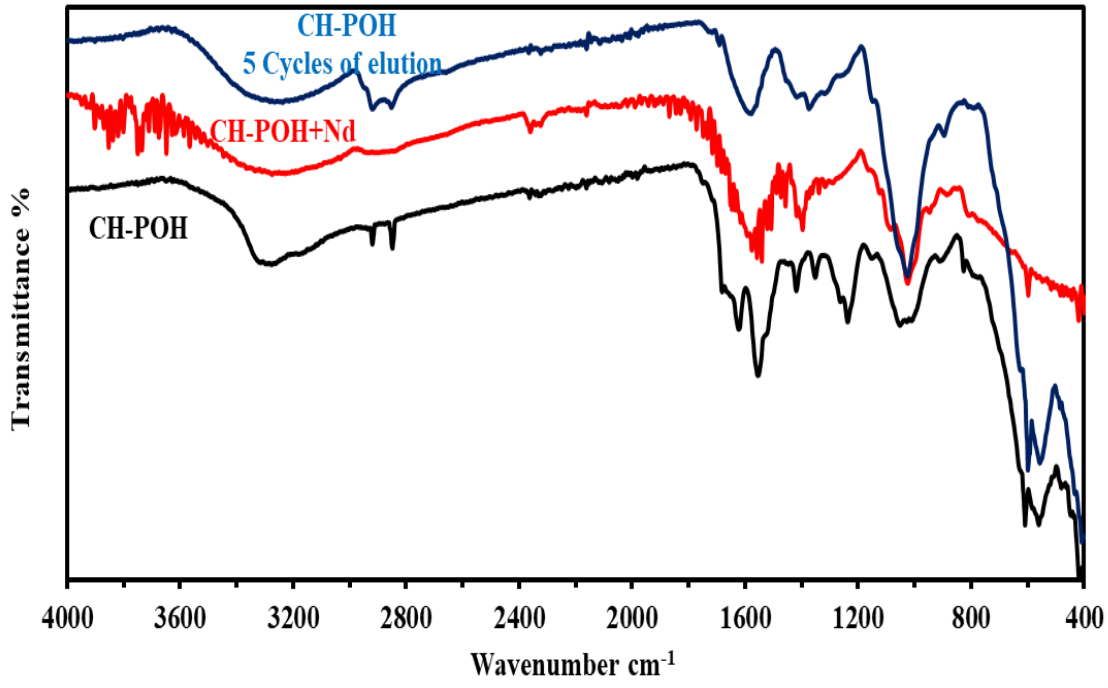

Figure S1. The full range of the FTIR spectra.

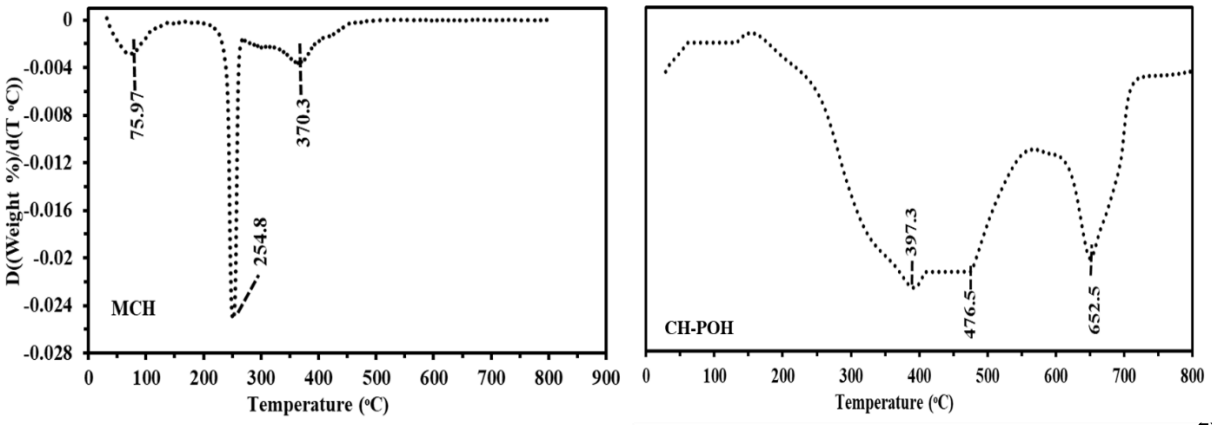

Figure S2. DrTG of chitosan magnetite (MCH) and functionalized sorbent (CH-POH)

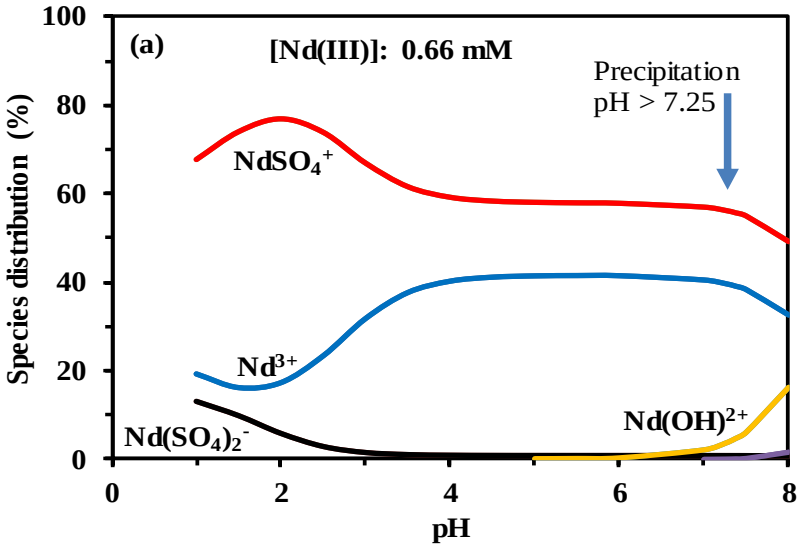

Figure S3. Speciation diagrams for Nd(III) under the experimental conditions

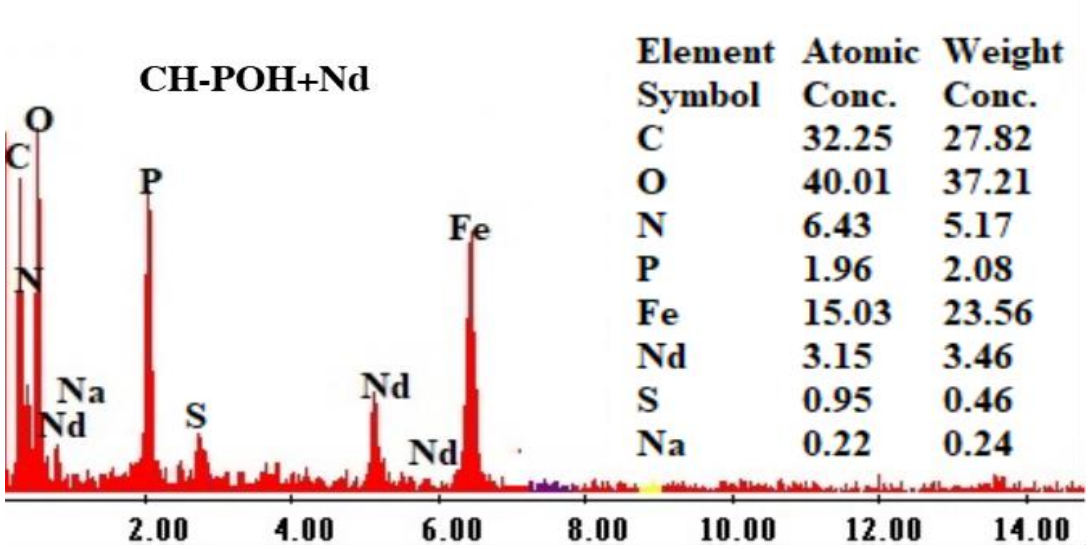

Element Symbol	Atomic Conc.	Weight Conc.
C	32.25	27.82
O	40.01	37.21
N	6.43	5.17
P	1.96	2.08
Fe	15.03	23.56
Nd	3.15	3.46
S	0.95	0.46
Na	0.22	0.24

Figure S4. EDX analysis of the CH-POH after Nd(III) sorption

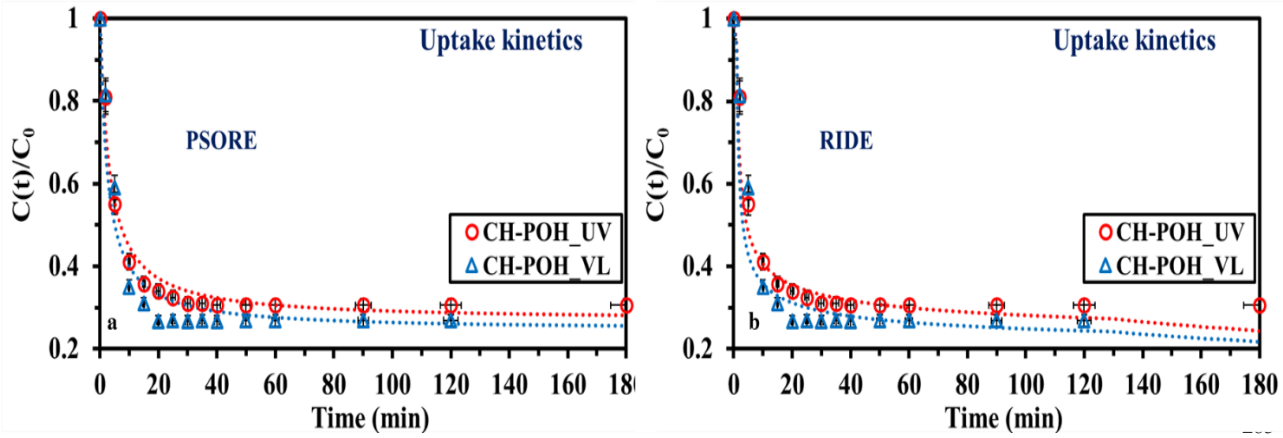

Figure S5. The unfitted profiles of the PSORE and RIDE for CH-POH sorbent, (pH_0: 4; C_0: 0.36 mmol Cd L^{-1}; SD: 0.66 g L^{-1}; T: 21 ±1 °C; v: 210 rpm).

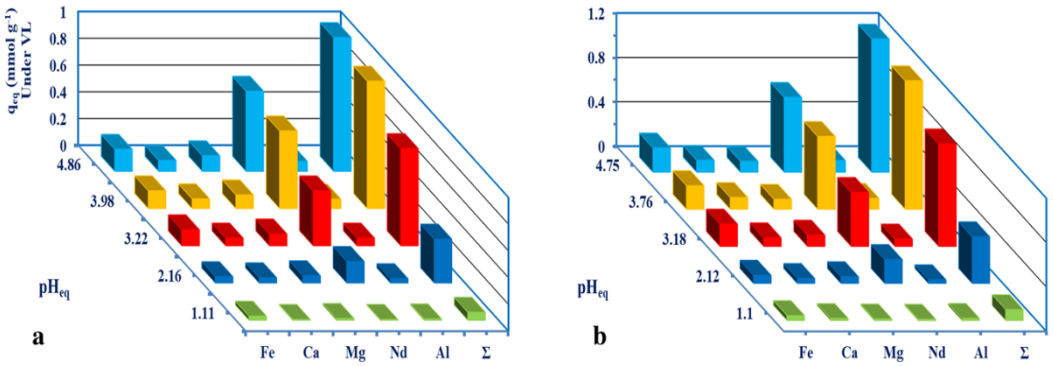

Figure S6. Total sorption capacity of CH-POH in polymetallic equimolar solution under VL(a) and (UV) conditions

Refrences

1. Hamza, M.F.; El Aassy, I.E.; Ahmed, F.Y.; Abdel-Rahman, A.A.-H.; Atta, A.M. Separation of uranium and rare earth elements with high purity from low-grade gibbsite-bearing shale ore by different chelating resins. *Journal of dispersion science and technology* **2012**, *33*, 482-489.
2. Fouda, A.; Salem, S.S.; Wassel, A.R.; Hamza, M.F.; Shaheen, T.I. Optimization of green biosynthesized visible light active CuO/ZnO nano-photocatalysts for the degradation of organic methylene blue dye. *Heliyon* **2020**, *6*, e04896.
3. Zhang, H.; Li, C.; Chen, X.; Fu, H.; Chen, Y.; Ning, S.; Fujita, T.; Wei, Y.; Wang, X. Layered ammonium vanadate nanobelt as efficient adsorbents for removal of Sr2+ and Cs+ from contaminated water. *Journal of Colloid and Interface Science* **2022**, *615*, 110-123.
4. Fouda, A.; Eid, A.M.; Guibal, E.; Hamza, M.F.; Hassan, S.E.-D.; Alkhalifah, D.H.M.; El-Hossary, D. Green Synthesis of Gold Nanoparticles by Aqueous Extract of Zingiber officinale: Characterization and Insight into Antimicrobial, Antioxidant, and In Vitro Cytotoxic Activities. *Applied Sciences* **2022**, *12*, 12879.
5. Chen, Y.; Ning, S.; Zhong, Y.; Li, Z.; Wang, J.; Chen, L.; Yin, X.; Fujita, T.; Wei, Y. Study on highly efficient separation of zirconium from scandium with TODGA-modified macroporous silica-polymer based resin. *Separation and Purification Technology* **2023**, *305*, 122499.
6. Hamza, M.F.; Salih, K.A.; Adel, A.-H.; Zayed, Y.E.; Wei, Y.; Liang, J.; Guibal, E. Sulfonic-functionalized algal/PEI beads for scandium, cerium and holmium sorption from aqueous solutions (synthetic and industrial samples). *Chemical Engineering Journal* **2021**, *403*, 126399.
7. Hamza, M.F.; Guibal, E.; Althumayri, K.; Vincent, T.; Yin, X.; Wei, Y.; Li, W. New Process for the Sulfonation of Algal/PEI Biosorbent for Enhancing Sr (II) Removal from Aqueous Solutions—Application to Seawater. *Molecules* **2022**, *27*, 7128.
8. Hamza, M.F.; Adel, A.-H.; Hawata, M.A.; El Araby, R.; Guibal, E.; Fouda, A.; Wei, Y.; Hamad, N.A. Functionalization of magnetic chitosan microparticles–Comparison of trione and trithione grafting for enhanced silver sorption and application to metal recovery from waste X-ray photographic films. *Journal of Environmental Chemical Engineering* **2022**, 107939.
9. Fouda, A.; Awad, M.A.; AL-Faifi, Z.E.; Gad, M.E.; Al-Khalaf, A.A.; Yahya, R.; Hamza, M.F. Aspergillus flavus-Mediated Green Synthesis of Silver Nanoparticles and Evaluation of Their Antibacterial, Anti-Candida, Acaricides, and Photocatalytic Activities. *Catalysts* **2022**, *12*, 462.
10. Fouda, A.; Eid, A.M.; Abdel-Rahman, M.A.; El-Belely, E.F.; Awad, M.A.; Hassan, S.E.-D.; Al-Faifi, Z.E.; Hamza, M.F. Enhanced antimicrobial, cytotoxicity, larvicidal, and repellence activities of brown algae, cystoseira crinita-mediated green synthesis of magnesium oxide nanoparticles. *Frontiers in Bioengineering and Biotechnology* **2022**, *10*.
11. Hamza, M.F.; Abu Khoziem, H.A.; Khalafalla, M.S.; Abdellah, W.M.; Zaki, D.I.; Althumayri, K.; Wei, Y. Ecofriendly Composite as a Promising Material for Highly-Performance Uranium Recovery from Different Solutions. *Toxics* **2022**, *10*, 490.
12. Fouda, A.; Hassan, S.E.-D.; Eid, A.M.; Awad, M.A.; Althumayri, K.; Badr, N.F.; Hamza, M.F. Endophytic bacterial strain, Brevibacillus brevis-mediated green synthesis of copper oxide nanoparticles, characterization, antifungal, in vitro cytotoxicity, and larvicidal activity. *Green Processing and Synthesis* **2022**, *11*, 931-950.
13. Hamza, M.F.; Mira, H.; Wei, Y.; Aboelenin, S.M.; Guibal, E.; Salem, W.M. Sulfonation of chitosan for enhanced sorption of Li (I) from acidic solutions–Application to metal recovery from waste Li-ion mobile battery. *Chemical Engineering Journal* **2022**, *441*, 135941.
14. Hamza, M.F.; Wei, Y.; Khalafalla, M.S.; Abed, N.S.; Fouda, A.; Elwakeel, K.Z.; Guibal, E.; Hamad, N.A. U (VI) and Th (IV) recovery using silica beads functionalized with urea-or thiourea-based polymers–Application to ore leachate. *Science of the Total Environment* **2022**, *821*, 153184.

15. Hamza, M.F.; Goda, A.E.-S.; Ning, S.; Mira, H.I.; Abdel-Rahman, A.A.-H.; Wei, Y.; Fujita, T.; Amer, H.H.; Alotaibi, S.H.; Fouda, A. Photocatalytic Efficacy of Heterocyclic Base Grafted Chitosan Magnetite Nanoparticles on Sorption of Pb (II); Application on Mining Effluent. *Catalysts* **2022**, *12*, 330.
16. Hamza, M.F.; Alotaibi, S.H.; Wei, Y.; Mashaal, N.M. High-Performance Hydrogel Based on Modified Chitosan for Removal of Heavy Metal Ions in Borehole: A Case Study from the Bahariya Oasis, Egypt. *Catalysts* **2022**, *12*, 721.
17. Fouda, A.; Hassan, S.E.-D.; Saied, E.; Hamza, M.F. Photocatalytic degradation of real textile and tannery effluent using biosynthesized magnesium oxide nanoparticles (MgO-NPs), heavy metal adsorption, phytotoxicity, and antimicrobial activity. *Journal of Environmental Chemical Engineering* **2021**, *9*, 105346.
18. Hamza, M.F.; Wei, Y.; Guibal, E. Quaternization of algal/PEI beads (a new sorbent): Characterization and application to scandium sorption from aqueous solutions. *Chemical Engineering Journal* **2020**, *383*, 123210.
19. Lin-Vien, D.; Colthup, N.B.; Fateley, W.G.; Grasselli, J.G. CHAPTER 16 - Organophosphorus Compounds. In *The Handbook of Infrared and Raman Characteristic Frequencies of Organic Molecules*, Lin-Vien, D., Colthup, N.B., Fateley, W.G., Grasselli, J.G., Eds.; Academic Press: San Diego, 1991; pp. 263-276.
20. Coates, J. Interpretation of Infrared Spectra, A Practical Approach. In *Encyclopedia of Analytical Chemistry* John Wiley & Sons, Ltd.: 2006; pp. 1-23.
21. Hamza, M.F.; Hamad, N.A.; Hamad, D.M.; Khalafalla, M.S.; Abdel-Rahman, A.A.-H.; Zeid, I.F.; Wei, Y.; Hessien, M.M.; Fouda, A.; Salem, W.M. Synthesis of eco-friendly biopolymer, alginate-chitosan composite to adsorb the heavy metals, Cd (II) and Pb (II) from contaminated effluents. *Materials* **2021**, *14*, 2189.
22. Hamza, M.F.; Mubark, A.E.; Wei, Y.; Vincent, T.; Guibal, E. Quaternization of composite algal/PEI beads for enhanced uranium sorption—application to ore acidic leachate. *Gels* **2020**, *6*, 12.
23. Hamza, M.F.; Fouda, A.; Wei, Y.; El Aassy, I.E.; Alotaibi, S.H.; Guibal, E.; Mashaal, N.M. Functionalized biobased composite for metal decontamination–Insight on uranium and application to water samples collected from wells in mining areas (Sinai, Egypt). *Chemical Engineering Journal* **2022**, *431*, 133967.
24. Hamza, M.F.; Sallam, O.R.; Khalafalla, M.S.; Abbas, A.E.A.; Wei, Y. Geological and radioactivity studies accompanied by uranium recovery: Um Bogma Formation, southwestern Sinai, Egypt. *Journal of Radioanalytical and Nuclear Chemistry* **2020**, *324*, 1039-1051.
25. Hamza, M.F. Grafting of quaternary ammonium groups for uranium (VI) recovery: Application on natural acidic leaching liquor. *Journal of Radioanalytical and Nuclear Chemistry* **2019**, *322*, 519-532.
26. Tien, C. *Adsorption Calculations and Modeling*; Butterworth-Heinemann: Newton, MA, 1994; p. 243.
27. Lima, É.C.; Dehghani, M.H.; Guleria, A.; Sher, F.; Karri, R.R.; Dotto, G.L.; Tran, H.N. CHAPTER 3 - Adsorption: Fundamental aspects and applications of adsorption for effluent treatment. In *Green Technologies for the Defluoridation of Water*, Hadi Dehghani, M., Karri, R., Lima, E., Eds.; Elsevier: 2021; pp. 41-88.
28. Buema, G.; Lupu, N.; Chiriac, H.; Ciobanu, G.; Bucur, R.D.; Bucur, D.; Favier, L.; Harja, M. Performance assessment of five adsorbents based on fly ash for removal of cadmium ions. *J. Mol. Liq.* **2021**, *333*, 115932, doi:10.1016/j.molliq.2021.115932.
29. Crank, J. *The Mathematics of Diffusion*, 2nd. ed.; Oxford University Press: Oxford, U.K., 1975; p. 414.
30. Ho, Y.S.; McKay, G. Pseudo-second order model for sorption processes. *Process Biochem.* **1999**, *34*, 451-465, doi:10.1016/S0032-9592(98)00112-5.